This document was prepared in conjunction with work accomplished under Contract No. AT(07-2)-1 with the U.S. Department of Energy.

DISCLAIMER

UNCLASSIFIED

TECHNICAL DIVISION
SAVANNAH RIVER LABORATORY

DPST-72-266

March 1, 1972

M E M O R A N D U M

TO: H. C. HONECK

FROM: H. L. DODDS
W. V. BAXTER
J. W. STEWART

ONE-DIMENSIONAL QUASISTATIC KINETICS*

SUMMARY

A comparison between the quasistatic method and the direct method of solving one-dimensional, zero-power reactor transient problems was made. Calculations were performed for a slab mockup of a heavily absorbing SRP production reactor using QX1 and ØDQ, both of which employ the improved quasistatic method, and WIGLE which utilizes a direct approach.

The results of the study support the following conclusions and observations:

(1) Each of the three codes accurately calculates one-dimensional, zero-power reactor transient problems.

(2) The solution obtained by the quasistatic method is a less sensitive function of the time interval between spatial calculations (i.e., has less error) than the solution obtained by the direct method. In other words, for comparable accuracy, larger time steps between spatial calculations can be used in the quasistatic method than in the direct method.

* The authors gratefully acknowledge M. Becker and D. A. Meneley for their interest and helpful suggestions during the course of this work.

(3) The code employing the direct method, WIGLE, required much less computer time for solving one-dimensional, two-energy group, zero-power reactor transient problems than the quasistatic code, QX1.

INTRODUCTION

Multi-dimensional reactor transient calculations utilizing the direct finite-difference method of solution are quite expensive when performed on the present generation of computers. In order to reduce computing costs without introducing unacceptable inaccuracies, more approximate methods of solution are being developed. One such method, proposed and being developed by Meneley and his associates at Argonne National Laboratory, is the "improved quasistatic" method.[1]

In this method, the space, energy, and time-dependent flux $\phi(\bar{r},E,t)$ is factored as follows:

$$\phi(\bar{r},E,t) = T(t)\ \psi(\bar{r},E,t)$$

where the shape function, $\psi(\bar{r},E,t)$ is a slowly varying function of time relative to the fast varying amplitude function, $T(t)$. The central idea of the quasistatic method is that $\psi(\bar{r},E,t)$ may be computed less often during the course of a transient than $\phi(\bar{r},E,t)$. Thus, a savings in computer time should be realized since a significant portion of any transient calculation is the time required to calculate the space- and energy-dependence of the neutron flux.

A primary consideration in the evaluation and subsequent implementation of any new method is accuracy. Meneley investigated the accuracy of the quasistatic method without feedback for both thermal and fast reactors having generation times ranging from 10^{-5} sec. to 3×10^{-7} sec. He found that, although the accuracy of the method was entirely adequate for all the cases that he considered, the error associated with the method was much larger for thermal systems with large generation times than for fast systems with small generation times.[1] A similar result was also found by Fuller.[2]

Hence, the primary objective of this work is to investigate the accuracy of the quasistatic method with respect to SRP reactors which have generation times of the order of 10^{-4} sec. In order to accomplish this objective, a comparison between calculations performed using the quasistatic method with calculations performed using a direct finite-difference (the so-called "exact" method) approach was made. Two codes employing the improved quasistatic method, ØDQ and QX1[3], and one code utilizing the direct method, WIGLE[4], were used in the investigation. QX1 and WIGLE are production status, one-dimensional codes originally developed at Argonne National Laboratory and Bettis Atomic Power Laboratory, respectively. ØDQ is a one-dimensional code developed at SRL for use as a research tool.

In this report, a description of the improved quasistatic method is presented. Calculational results, which illustrate the accuracy of the method, are presented for two types of perturbations - a highly localized perturbation and a nearly uniform perturbation. Execution times for the two production codes, QX1 and WIGLE, are also presented.

THE QUASISTATIC METHOD

The improved quasistatic kinetics method is an approximate method for solving the following equations:

$$\underline{\underline{V}}^{-1} \frac{\partial}{\partial t} \underline{\phi}(\bar{r},t) = \left[\nabla \cdot \underline{\underline{D}}(\bar{r},t)\nabla - \underline{\underline{A}}(\bar{r},t) + (1-\beta)\underline{\chi}_p \underline{F}^T(\bar{r},t)\right] \underline{\phi}(\bar{r},t) \qquad (1)$$

$$+ \sum_{i=1}^{M} \underline{\chi}_i \lambda_i C_i(\bar{r},t) + \underline{S}(\bar{r},t)$$

$$\frac{\partial}{\partial t} C_i(\bar{r},t) = \beta_i \underline{F}^T(\bar{r},t)\underline{\phi}(\bar{r},t) - \lambda_i C_i(\bar{r},t) \quad i = 1,\ldots,M \qquad (2)$$

where $\bar{r}$ is the position vector, t is time, and $\underline{\underline{V}}^{-1}$ is a G x G diagonal matrix containing the inverse velocities for G energy groups. A doubly underlined quantity denotes G x G square matrix, a singly underlined quantity denotes G x 1 matrix, and a scalar is denoted by a quantity with no underline. $\underline{\phi}$ is the flux vector, $\underline{\underline{D}}$ is the diffusion coefficient (diagonal) matrix, and $\underline{\underline{A}}$ is the removal plus inscattering matrix. β is the delayed neutron fraction, $\underline{\chi}_p$ is the prompt neutron fission spectrum, and $\underline{F}^T$ denotes the transpose of the production cross section vector. M denotes the number of delayed neutron precursor families, $\underline{\chi}_i$ is the delayed neutron fission spectrum, and λ_i is the decay constant for precursor family i. C_i is precursor density for precursor family i, $\underline{S}$ is the external neutron source vector, and β_i is the delayed neutron fraction for precursor family i.

The quasistatic method can also be used to solve the thermal/hydraulic equations simultaneously with the above neutronic equations. However, this work is concerned only with the neutronic equations.

The fundamental assumption in the quasistatic method is that the flux vector may be separated into a shape function that is slowly varying with time, $\underline{\psi}(\bar{r},t)$, and a more rapidly varying amplitude function, T(t), as shown below:

$$\underline{\phi}(\bar{r},t) = \underline{\psi}(\bar{r},t)\, T(t) \qquad (3)$$

with*

$$\frac{1}{P}\left\langle \underline{\omega}(\bar{r},t),\ \underline{\underline{V}}^{-1}\ \underline{\psi}(\bar{r},t)\right\rangle = \text{constant} = \gamma \qquad (4)$$

where P is adjusted so that $\gamma = 1$ at $t = 0$. $\underline{\omega}$ is a weight function that is usually selected to be the unperturbed steady state adjoint solution of Equation (1). Equation (4) determines uniquely the separation indicated by Equation (3). More importantly, the condition that $\gamma \cong 1$ for all time provides a constraint which must be satisfied throughout the transient.

The central idea in the quasistatic method is that a low order approximation with large integration time steps may be used for the calculation of $\underline{\psi}(\bar{r},t)$; whereas, a high order approximation with small integration time steps is used for the calculation of $T(t)$. The separation indicated by Equation (3) should permit the use of larger time steps for the calculation of $\underline{\psi}(\bar{r},t)$ than would be required for the calculation of $\underline{\phi}(r,t)$. Thus, since a very time-consuming portion of any space-time transient calculation is the spatial calculation at each time step, a reduction in the computation time per transient should be realized provided the additional computation time required for the calculation of $T(t)$ and also the time required to satisfy the constraint equation are not significant. Substitution of Equations (3) and (4) into Equations (1) and (2) yields, after some rearrangement, the following equations:

$$\frac{d}{dt}T(t) = \left(\frac{\rho(t) - \bar{\beta}(t)}{\Lambda(t)}\right)T(t) + \sum_{i=1}^{M}\lambda_i\ \xi_i(t) + Q(t) \qquad (5a)$$

$$\frac{d}{dt}\xi_i(t) = \frac{\beta_i(t)}{\Lambda(t)}T(t) - \lambda_i\xi_i(t) \qquad i = 1,\ldots,M \qquad (5b)$$

where:

$$\frac{\rho}{\Lambda} = \frac{1}{E}\left\langle \underline{\omega}, \left\{\nabla\cdot\underline{\underline{D}}\nabla - \underline{\underline{A}} + \left[(1-\beta)\chi_p + \sum_{i=1}^{M}\beta_i\chi_i\right]\underline{\underline{F}}^T\right\}\underline{\psi}\right\rangle$$

$$\frac{\bar{\beta}}{\Lambda} = \sum_{i=1}^{M}\frac{\bar{\beta}_i}{\Lambda} = \sum_{i=1}^{M}\frac{1}{E}\left\langle \underline{\omega}, \beta_i\chi_i\underline{\underline{F}}^T\underline{\psi}\right\rangle$$

---

* The brackets indicate an inner product defined as

$$\left\langle \underline{\omega}, \underline{\underline{\Theta}}\underline{Z}\right\rangle = \int_{\text{Volume}} (\omega_1\ldots\omega_G)\begin{pmatrix}\Theta_{11}\cdots\Theta_{1G}\\ \vdots\quad\ \vdots\\ \Theta_{G1}\cdots\Theta_{GG}\end{pmatrix}\begin{pmatrix}Z_1\\ \vdots\\ Z_G\end{pmatrix} d\bar{r}$$

$$\xi_i = \frac{1}{E}\left\langle \underline{\omega}, \underline{\underline{I}}\ \underline{\chi}_i C_i \right\rangle, \quad Q = \frac{1}{E}\left\langle \underline{\omega}, \underline{\underline{I}} S \right\rangle$$

$$E = \langle \gamma P = \left\langle \underline{\omega}, \underline{\underline{V}}^{-1}\ \underline{\psi} \right\rangle = \text{constant}$$

$$C_i(\bar{r},t) = \beta_i \int_{t_0}^{t} \underline{F}^T(\bar{r},t')\ \underline{\phi}(\bar{r},t')\ e^{-\lambda_i(t-t')}\, dt'$$

$$+ e^{-\lambda_i(t-t_0)}\, C_i(\bar{r},t_0)\ , \quad i = 1,\ldots,M \tag{6}$$

$$\underline{\underline{V}}^{-1}\ \frac{\partial}{\partial t}\ \underline{\psi} + \underline{\underline{V}}^{-1}\ \underline{\psi}\ \frac{1}{T}\frac{dT}{dt} = \left[\nabla \cdot \underline{\underline{D}} \nabla - \underline{\underline{A}} + (1-\beta)\ \underline{\chi}_p \underline{F}^T\right]\ \underline{\psi}$$

$$+ \frac{1}{T}\sum_{i=1}^{M} \underline{\chi}_i\ \lambda_i\ C_i + \frac{1}{T}\ \underline{S} \tag{7}$$

Thus, instead of solving Equations (1) and (2) directly, the quasi-static approach is to solve Equations (5), (6), and (7) along with the constraint equation, Equation (4). It is important to note that no approximations have been made thus far. Next consider the numerical solution of Equations (4-7).

Numerical Solution of Equations (4-7)

Equations (4-7) are solved numerically using a hierarchy of three different integration time intervals, $\Delta t^k \in \Delta t^j \in \Delta t^B$, as shown below:

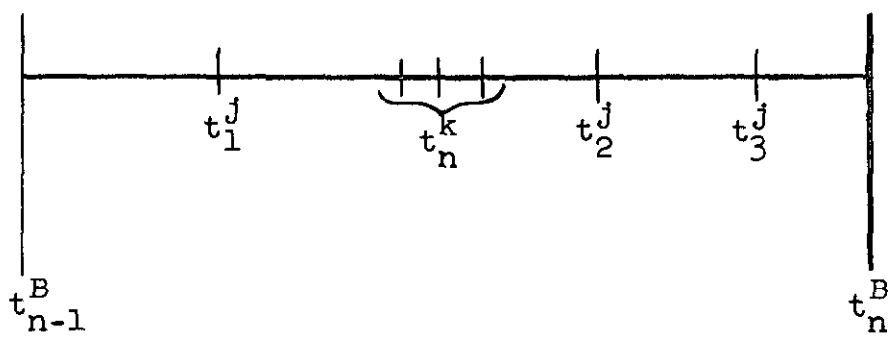

The shape function $\underline{\psi}(\bar{r},t)$ is assumed to vary linearly over the largest time interval, $\Delta t_n^B = t_n^B - t_{n-1}^B$. A simple backward difference in time is used to approximate Equation (7) which gives the following:

$$\left\{ -\nabla\cdot\underline{\underline{D}}\nabla + \underline{\underline{A}} - (1-\beta)\,\underline{\chi}_p\,\underline{F}^T + \underline{\underline{V}}^{-1}\left[\frac{1}{T}\frac{dT}{dt} + \frac{1}{\Delta t^B}\right]\right\}_{t_n^B} \underline{\psi}(\bar{r},t_n^B)$$

$$= \frac{1}{\Delta t^B}\,\underline{\underline{V}}^{-1}\,\underline{\psi}(\bar{r},t_{n-1}^B) + \left\{\frac{1}{T}\sum_{i=1}^{M}\underline{\chi}_i\lambda_i C_i + \frac{1}{T}\,\underline{S}\right\}_{t_n^B} \qquad (8a)$$

In shorthand notation Equation (8a) becomes

$$\underline{\underline{O}}\,\underline{\psi}(\bar{r},t_n^B) = \underline{Z} \qquad (8b)$$

where definitions of the operator $\underline{\underline{O}}$ and the driving function $\underline{Z}$ are obvious from comparing (8a) and (8b).

In Equation (6), the fission density $\underline{F}^T\underline{\phi}$ is assumed to vary linearly over $\Delta t_n^j = t_n^j - t_{n-1}^j$ which gives the following, using $\underline{\phi} = \underline{\psi}\,T$,

$$C_i(\bar{r},t_n^j) = \beta_i\left[a_i^n\underline{F}^T(\bar{r},t_n^j)\,\underline{\psi}(\bar{r},t_n^j) + b_i^n\underline{F}^T(\bar{r},t_{n-1}^j)\underline{\psi}(\bar{r},t_{n-1}^j)\right]$$

$$+ e^{-\lambda_i(t_n^j - t_{n-1}^j)}\,C_i(\bar{r},t_{n-1}^j) \qquad i = 1,\ldots,M \qquad (9)$$

where:

$$a_i^n = \frac{1}{t_n^j - t_{n-1}^j}\int_{t_{n-1}^j}^{t_n^j} e^{-\lambda_i(t_n^j - t')}\,(t' - t_{n-1}^j)\,T(t')\,dt'$$

$$b_i^n = \frac{1}{t_n^j - t_{n-1}^j}\int_{t_{n-1}^j}^{t_n^j} e^{-\lambda_i(t_n^j - t')}\,(t_n^j - t')\,T(t')\,dt'$$

The a_i^n and b_i^n above are evaluated simultaneously with the solution of Equations (5a) and (5b) using a fourth order Runge-Kutta approximation over the Δt^k time intervals. Values for the coefficients, ρ, $\bar{\beta}_j$, $\bar{\beta}_1$, and Λ are computed using their inner product definitions at the t^j time points. Quadratic interpolation is used to obtain intermediate values of the coefficients at the t^k time points.

Equation (8b) is solved in a somewhat unusual manner which involves the use of Equation (4).

Specifically, expand $\underline{\underline{O}}$ as $\underline{\underline{O}}^1 - \underline{\underline{O}}^2$ where

$$\underline{\underline{O}}^1 = \left\{ \nabla \cdot \underline{\underline{D}} \nabla - \underline{\underline{A}} + \underline{\underline{V}}^{-1} \left[\frac{1}{T} \frac{dT}{dt} + \frac{1}{\Delta t^B} \right] \right\}_{t_n^B}$$

$$\underline{\underline{O}}^2 = \left\{ (1 - \beta)\, \underline{\chi}_p\, \underline{F}^T \right\}_{t_n^B} .$$

Therefore, Equation (8b) becomes

$$\underline{\underline{O}}^1\, \underline{\psi}(\bar{r}, t_n^B) = \underline{\underline{O}}^2\, \underline{\psi}(\bar{r}, t_n^B) + \underline{Z} .$$

A conventional iterative approach for solving the above equation is as follows:

$$\underline{\underline{O}}^1\, \underline{\psi}^{\ell+1} = \frac{\underline{\underline{O}}^2\, \underline{\psi}^{\ell}}{\alpha^{\ell}} + \underline{Z} \qquad (10a)$$

where ℓ is the iteration index and

$$\alpha^{\ell} = \frac{\langle \underline{1}, \underline{\underline{O}}\, \underline{\psi}^{\ell} \rangle}{\langle \underline{1}, \underline{\underline{I}}\, \underline{Z} \rangle} \qquad (10b)$$

with $\underline{1} = (1 \ldots 1)^T$.

As discussed by Meneley,[3] numerical difficulties are encountered when using the above procedure for transients in the neighborhood of prompt critical. In order to circumvent this problem, Meneley proposed the following procedure which utilizes Equation (4).

$$\underline{\underline{O}}^1\, \underline{\psi}^{\ell+1} = \underline{\underline{O}}^2\, \frac{\underline{\psi}^{\ell}}{\gamma^{\ell}} + \underline{Z} \qquad (11a)$$

where

$$\gamma^{\ell} = \left\langle \underline{w}, \underline{\underline{V}}^{-1} \underline{\psi}^{\ell} \right\rangle \Big/ P \qquad (11b)$$

Note that the ℓ iteration in the above procedure results in a converged value of γ and a converged shape function $\underline{\psi}$. This procedure has been implemented successfully in the QX1 and ØDQ codes. For a more detailed discussion of this procedure see Reference (3).

A general description of the solution algorithm is outlined below:

1. Assume everything is known at time t^B_{n-1}.
2. Extrapolate $\underline{\psi}$ linearly with respect to time from $\underline{\psi}(\bar{r},t^B_{n-1})$ to $\underline{\psi}(\bar{r},t^B_n)$.
3. Evaluate ρ, $\bar{\beta}$, Λ, $\bar{\beta}_i$ at t^j_1 using their inner product definitions.
4. Interpolate ρ, $\bar{\beta}$, Λ, $\bar{\beta}_i$ between t^B_{n-1} and t^j_1 at the t^k points.
5. Solve Equation (5) and evaluate a^n_i, b^n_i out to t^j_1 .
6. Update $C_i(\bar{r},t)$ to $t = t^j_1$ using Equation (9).
7. If $t^j_1 < t^B_n$, go to next t^j point and repeat steps 3 - 6.
8. If $t^j_1 = t^B_n$, solve Equation (11) for a new $\underline{\psi}(\bar{r},t^B_n)$ and a new γ.
9. If $\gamma_{new} = 1$, go to the next Δt^B interval and repeat steps 2 - 8.
10. If $\gamma_{new} \neq 1$, replace $\underline{\psi}(\bar{r}, t^B_n)$ with the new $\underline{\psi}(\bar{r},t^B_n)$ and repeat steps 2 - 10 for the same Δt^B interval, or repeat steps 2 - 10 for a shorter Δt^B interval.

DISCUSSION OF RESULTS AND CONCLUSIONS

A comparison between results obtained with the two quasistatic codes, QX1 and ØDQ, with results obtained with WIGLE was made for the one-dimensional slab reactor shown in Figure 1. The steady-state, two-group parameters that were used are presented in Table I. This particular reactor is representative of a somewhat heavy SRP lattice which has a generation time of 1.74×10^{-4} sec. For the first two transients, the perturbation was initiated by decreasing the thermal group capture cross section in Region 3.

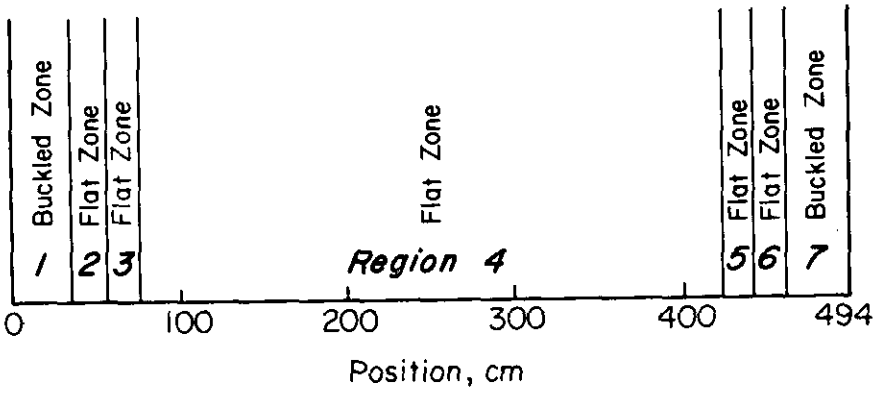

FIG. 1 SLAB MOCKUP OF A HEAVILY ABSORBING SRP PRODUCTION REACTOR

TABLE I

UNPERTURBED TWO GROUP PARAMETERS FOR PRODUCTION REACTOR MOCKUP (TRANSVERSE BUCKLING - 50 μB)

	Group i	D^i	Σ_r^i	$\Sigma_s^{i\to j}$	$\nu\Sigma_f^i$	Σ_c^i
Buckled Zone	1	1.385	.010796	.008547	.0020927	.001401
	2	.8792	.018100	-0-	.026304	.009802
Flat Zone	1	1.385	.010796	.008547	.0020917	.001401
	2	.8792	.019778	-0-	.020348	.01148

$$\Sigma_r^i = \Sigma_c^i + \Sigma_f^i + \Sigma_s^{i\to j}, \quad V_1^{-1} = 10^{-7}, \; V_2^{-1} = 4.04 \times 10^{-6}$$

DELAYED NEUTRON PARAMETERS

GROUP	β_i	$\lambda_i (sec^{-1})$
1	.0009856	1.55
2	.0043140	.209
3	.0017650	.0247
4	.00008052	.00280
5	.00003679	.000147
6	.00000119	.00000141

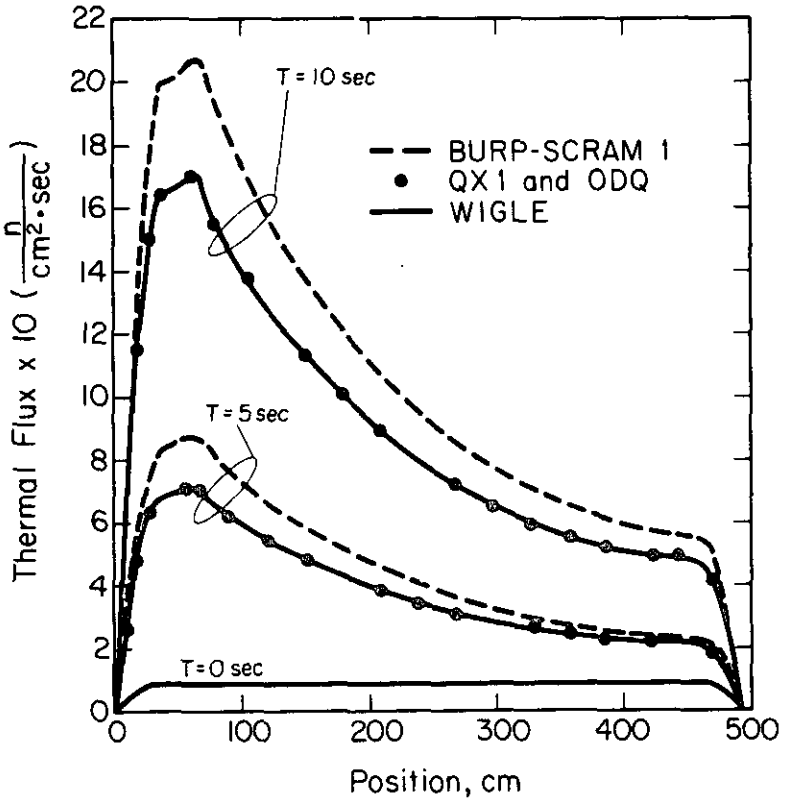

FIG. 2 RESPONSE DUE TO STEP CHANGE IN Σ_c^2 IN REGION 3
($\Delta\Sigma_c^2$ = -0.00125)

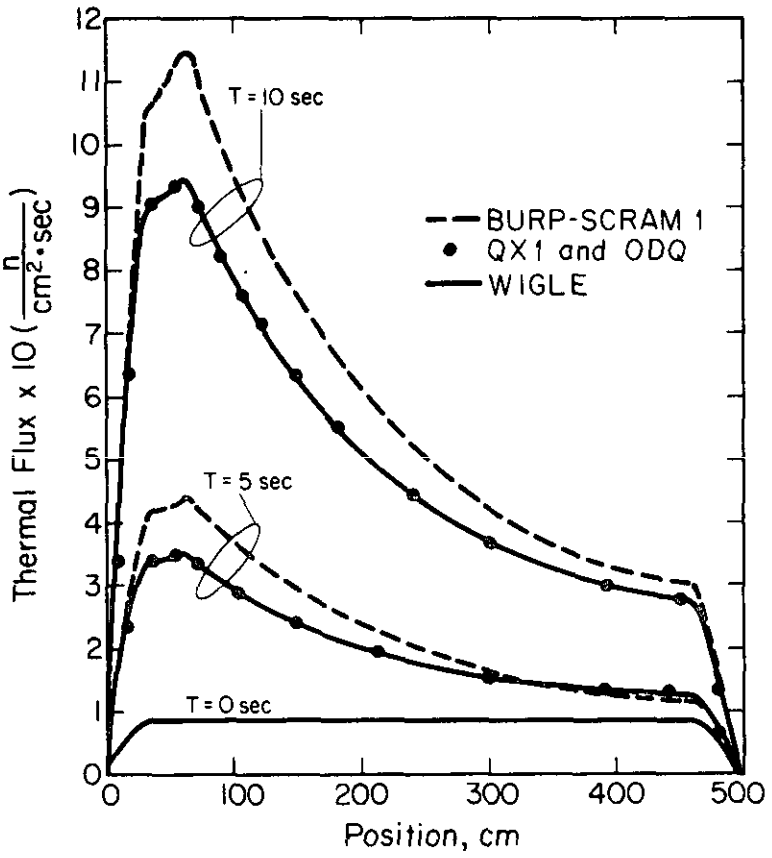

FIG. 3 RESPONSE DUE TO 5-SEC RAMP IN Σ_c^2 IN REGION 3
($\Delta\Sigma_c^2$ = -0.00125)

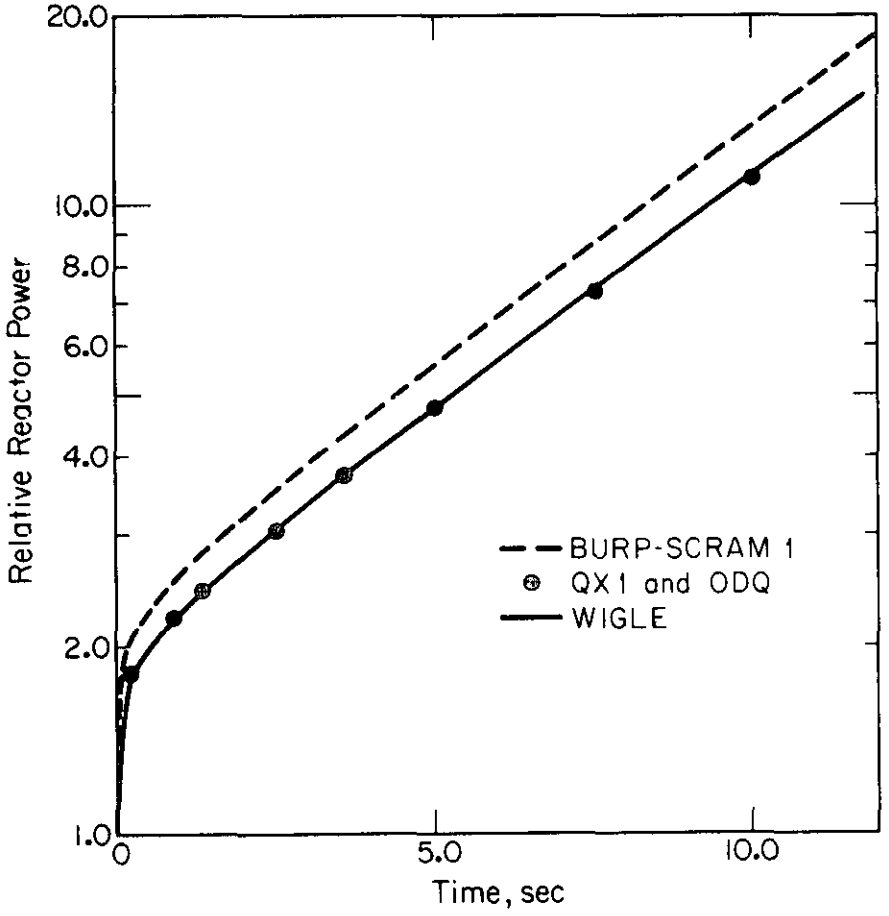

FIG. 4 REACTOR POWER RESPONSE TO STEP CHANGE IN Σ_c^2 IN REGION 3 ($\Delta\Sigma_c^2$ = -0.00125)

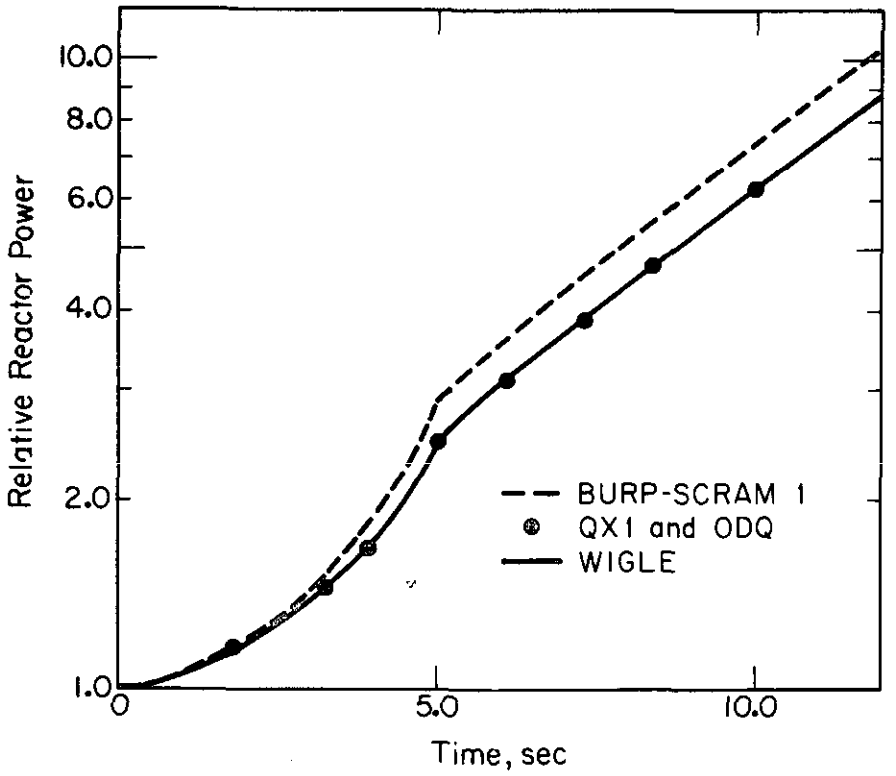

FIG. 5 REACTOR POWER RESPONSE TO 5-SEC RAMP IN Σ_c^2 IN REGION 3 ($\Delta\Sigma_c^2$ = -0.00125)

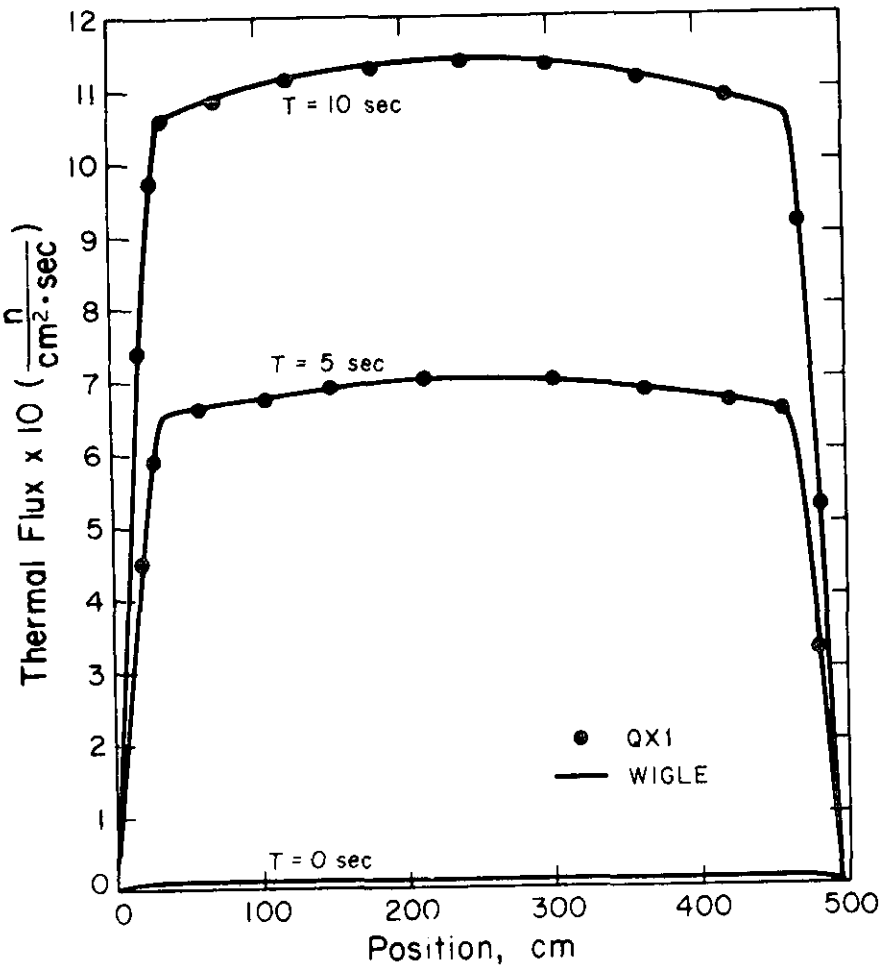

FIG. 6 RESPONSE DUE TO 5-SEC RAMP IN Σ_c^2 IN REGIONS 2-6 ($\Delta\Sigma_c^2$ = -0.00014062)

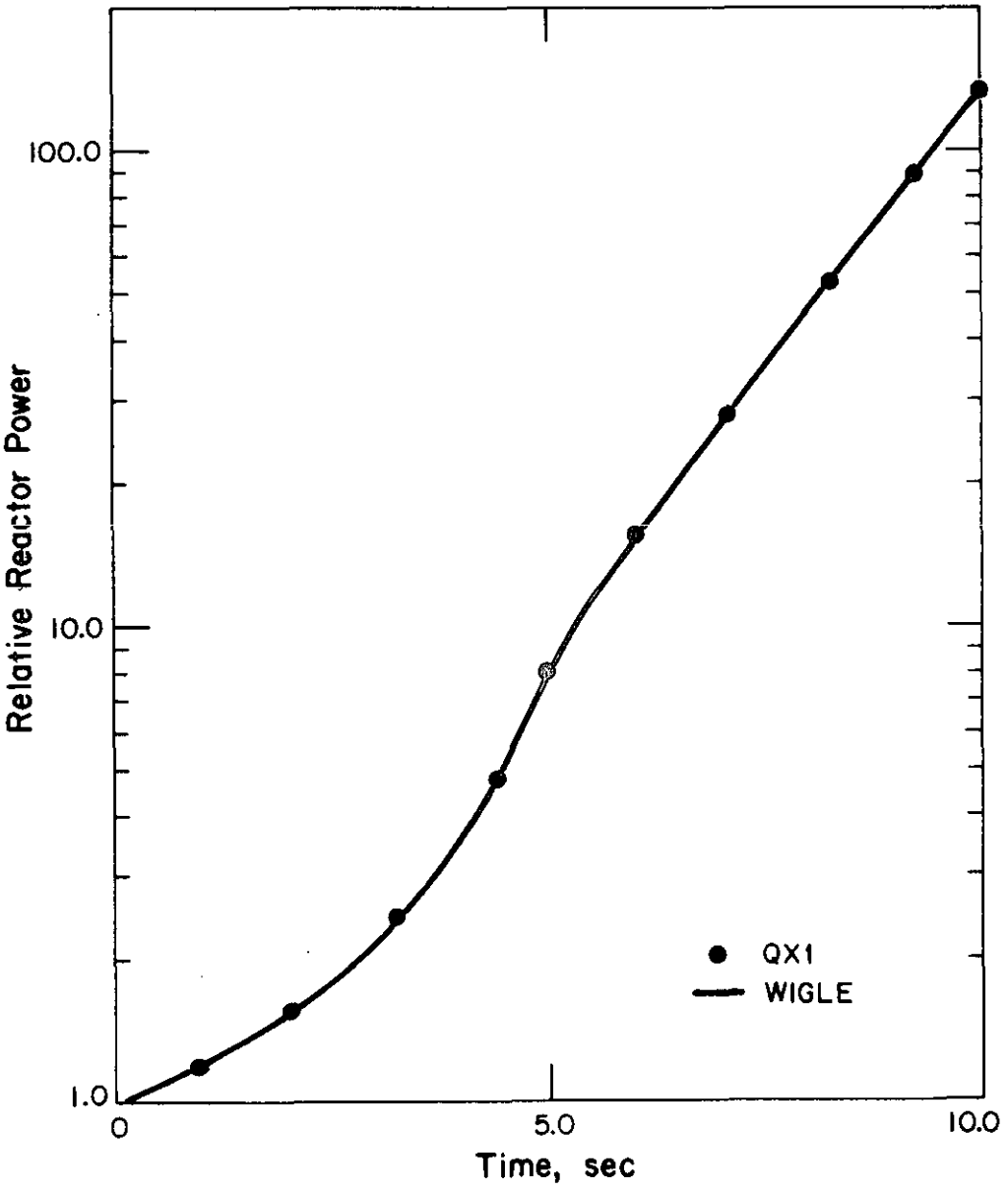

FIG. 7 REACTOR POWER RESPONSE TO 5-SEC RAMP IN Σ_c^2 IN REGIONS 2-6 ($\Delta\Sigma_c^2$ = -0.00014062)

In all of the calculations described above, the "average" time interval between spatial (and energy) calculations was small - approximately .02 seconds. An "average" time interval is reported since QX1 has an automatic time step algorithm which selects the points in time, non-uniformly, at which the shape function is to be calculated.

In order to obtain more detailed information on the accuracy of the quasistatic method versus the direct method, the sensitivity of each solution to the average time interval between spatial calculations was investigated. The power at 5 seconds and the power at 10 seconds versus the average time interval between spatial calculations are presented in Figures 8 and 9, respectively, for the transient initiated by a 5-second ramp in Σ^{th}_{c} in Region 3. The same information for the transient initiated by the nearly uniform perturbation is presented in Figures 10 and 11. As may be observed in each of the four figures, the quasistatic solution is less sensitive to the average time interval than the direct solution. In other words, for the same average time interval between spatial calculations, the error associated with the quasistatic method is less than the error associated with the direct method.

Finally, as additional information, the computer running time (i.e., CPU time) versus the average time interval between spatial calculations is presented in Figures 12 and 13 for two of the transients discussed above. From the results presented, it is obvious that WIGLE is considerably more efficient than QX1 for solving the type of problems considered in this work; namely, one-dimensional, two-group, reactor transient problems with no engineering feedback. However, a careful distinction should be made at this point between efficiency of codes and efficiency of methods. QX1 is a multigroup (up to 30 energy groups) code which includes, in addition to the neutronics model, an elaborate engineering feedback model that is characteristic of an LMFBR. WIGLE is strictly a two-group code with an unsophisticated feedback model. QX1 has a generalized, automatic time step selector; whereas, in WIGLE, the time steps are input by the user. These differences, as well as programming efficiency, in the two codes, cause a difference in computational time.

An example of one methodical difference which affects the computation time comparison is the way QX1 performs a spatial calculation at each time step versus the way WIGLE performs the same calculation at each time step. Because WIGLE is only a two-group code, it uses a non-iterative technique to perform the spatial calculation at each time step as opposed to QX1 which uses an iterative technique to solve the same type of problem simply because QX1 must be able to handle up to 30 energy groups. In other words, the QX1 iterative method is less efficient for performing a two-group spatial calculation than the non-iterative WIGLE method.

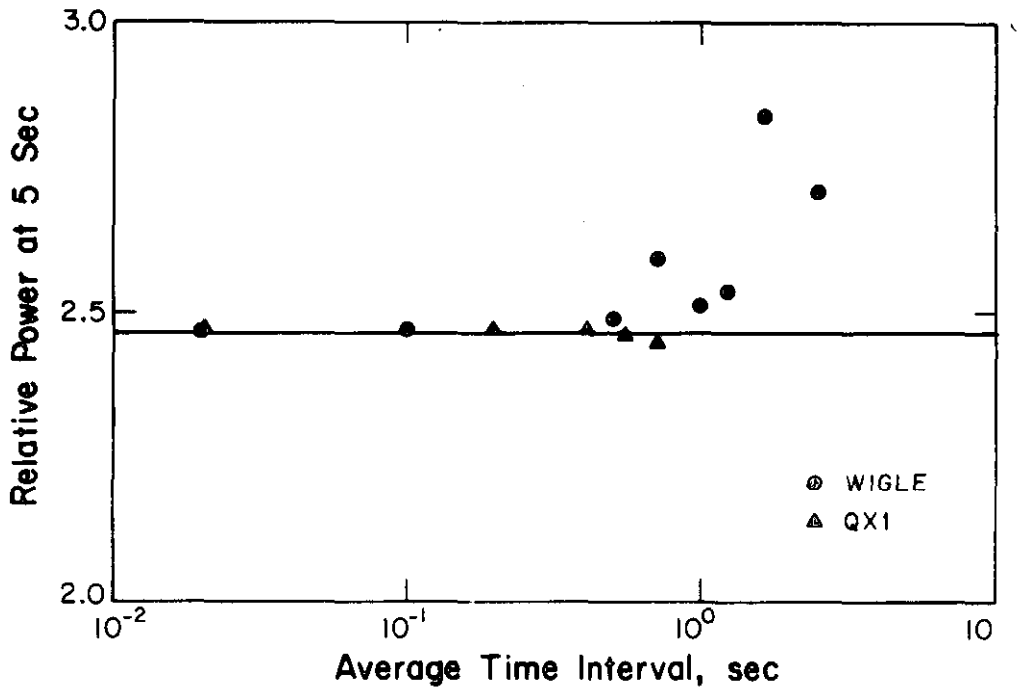

FIG. 8 POWER AT 5 SEC VERSUS AVERAGE TIME INTERVAL BETWEEN SPATIAL CALCULATIONS FOR A 5-SEC RAMP PERTURBATION IN Σ_c^2 IN REGION 3

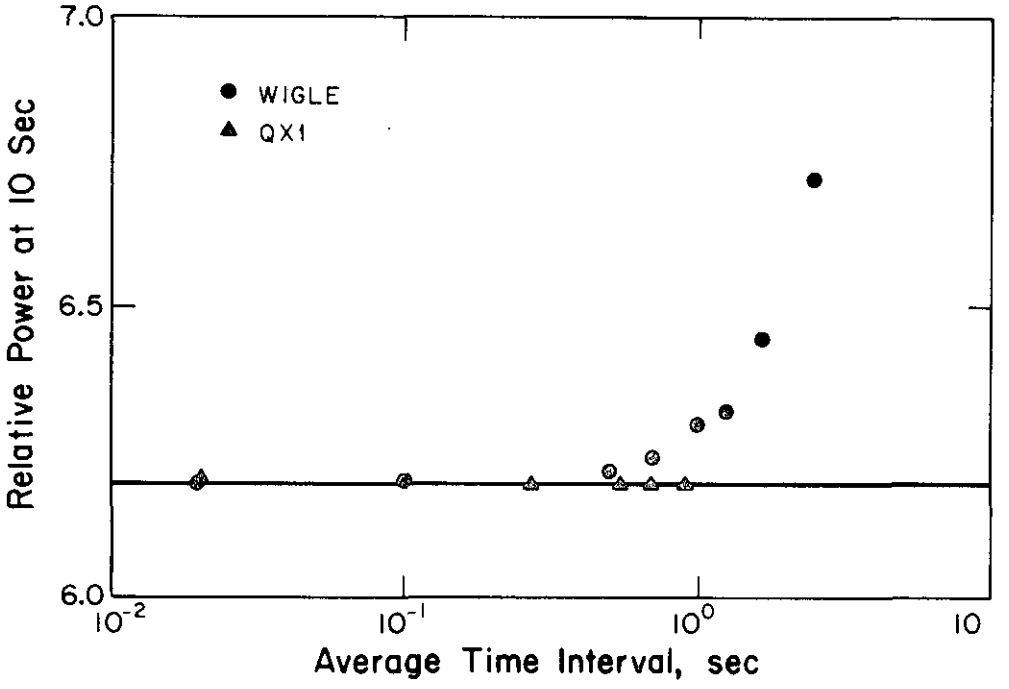

FIG. 9 POWER AT 10 SEC VERSUS AVERAGE TIME INTERVAL BETWEEN SPATIAL CALCULATIONS FOR A 5-SEC RAMP PERTURBATION IN Σ_c^2 IN REGION 3

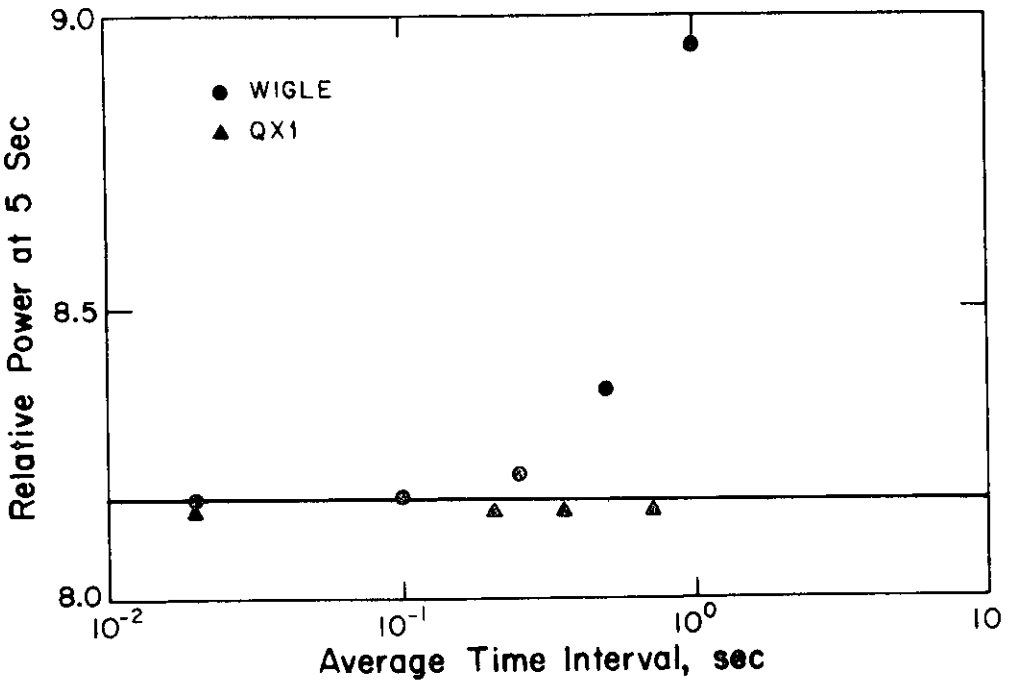

FIG. 10 POWER AT 5 SEC VERSUS AVERAGE TIME INTERVAL BETWEEN SPATIAL CALCULATIONS FOR A 5-SEC RAMP PERTURBATION IN Σ_c^2 IN REGIONS 2-6

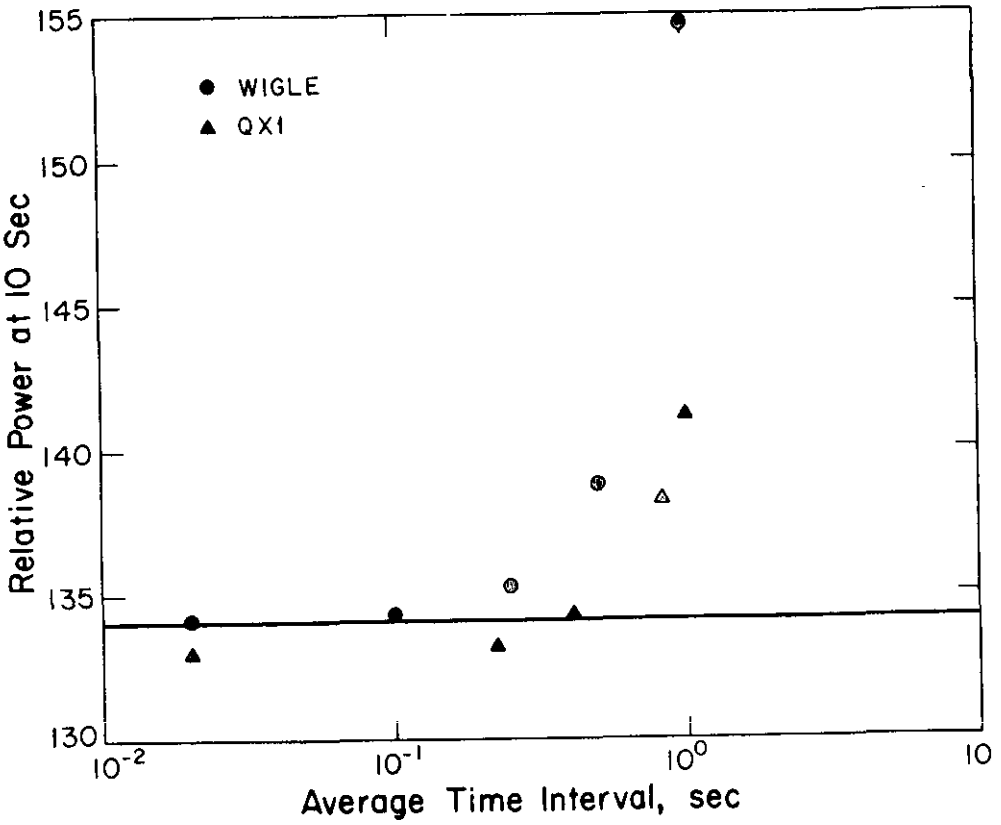

FIG. 11 POWER AT 10 SEC VERSUS AVERAGE TIME INTERVAL BETWEEN SPATIAL CALCULATIONS FOR A 5-SEC RAMP PERTURBATION IN Σ_c^2 IN REGIONS 2-6

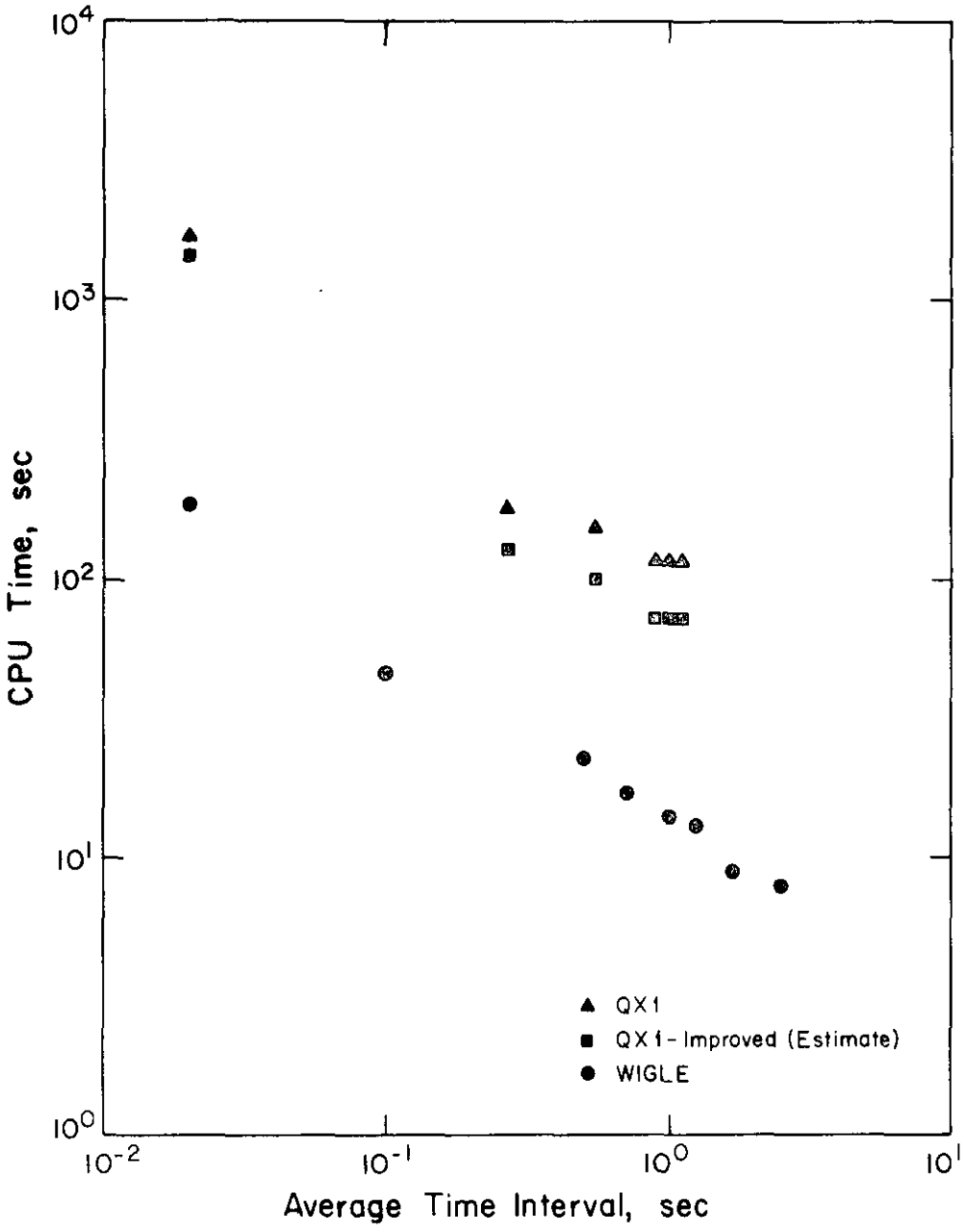

FIG. 12 CPU TIME VERSUS AVERAGE TIME INTERVAL BETWEEN SPATIAL CALCULATIONS FOR A 10-SEC TRANSIENT (5-SEC RAMP PERTURBATION IN Σ_c^2 IN REGION 3)

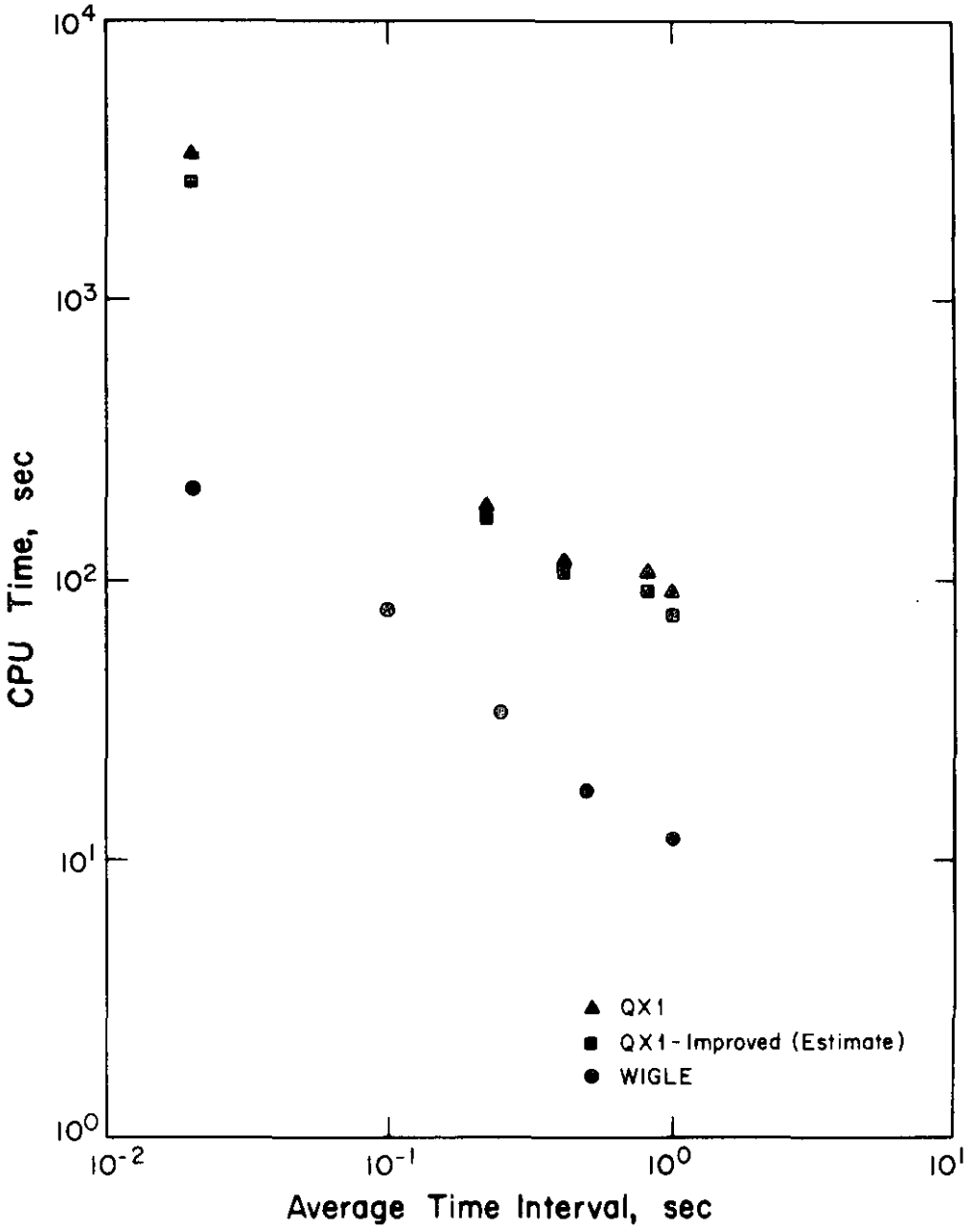

FIG. 13 CPU TIME VERSUS AVERAGE TIME INTERVAL BETWEEN SPATIAL CALCULATIONS FOR A 10-SEC TRANSIENT (5-SEC RAMP PERTURBATION IN Σ_c^2 IN REGIONS 2-6)

In order to ascertain the improvement in the QX1 running time which would occur if QX1 used the non-iterative WIGLE technique to perform the spatial calculation, a CPU timer was employed in each code to measure the actual time that each spent in doing the spatial calculations. This information was then used to obtain an estimate of the computation time that QX1 would require if it utilized the non-iterative technique employed in WIGLE. The results are presented in Figures 12 and 13. Note that the improvement in QX1 computation time is more significant for the transient initiated by the localized perturbation than for the transient initiated by the nearly uniform perturbation. Nevertheless, there still remains sufficient differences in the two codes that WIGLE is definitely more economical than QX1 for solving one-dimensional, two-group problems with no engineering feedback.

HLD:msg

REFERENCES:

(1) K. O. Ott and D. A. Meneley, "Accuracy of the Quasistatic Treatment of Spatial Reactor Kinetics," Nuclear Science & Engineering, 36, 402 (1969).

(2) E. L. Fuller, "One-Dimensional Thermal Reactor Kinetics Benchmark Calculations," Transactions of the American Nuclear Society, 14, 233 (1970).

(3) D. A. Meneley, K. O. Ott, and E. S. Wiener, "Fast-Reactor Kinetics - The QX1 Code," ANL-7769, Argonne National Laboratory (March, 1971).

(4) J. W. Stewart, Module WIGLE, The JOSHUA System, DPSTM-500, Vol. VII, E. I. du Pont, Savannah River Laboratory.

(5) P. B. Parks, "Comparison of Adiabatic and Direct Space-Time Neutronics Models," DPST-70-561 (unpublished SRL memorandum), Savannah River Laboratory (December, 1970).